Development 139, 2246-2253 (2012) doi:10.1242/dev.080275

Chemokine and Fgf signalling act as opposing guidance cues in formation of the lateral line primordium

Marie A. Breau, Duncan Wilson, David G. Wilkinson and Qiling Xu*

SUMMARY

The directional migration of many cell populations occurs as a coherent group. An amenable model is provided by the posterior lateral line in zebrafish, which is formed by a cohesive primordium that migrates from head to tail and deposits future neuromasts at intervals. We found that prior to the onset of migration, the compact state of the primordium is not fully established, as isolated cells with lateral line identity are present caudal to the main primordium. These isolated cells are retained in position such that they fuse with the migrating primordium as it advances, and later contribute to the leading zone and terminal neuromasts. We found that the isolated lateral line cells are positioned by two antagonistic cues: Fgf signalling attracts them towards the primordium, which counteracts Sdf1α/Cxcr4b-mediated caudal attraction. These findings reveal a novel chemotactic role for Fgf signalling in which it enables the coalescence of the lateral line primordium from an initial fuzzy pattern into a compact group of migrating cells.

KEY WORDS: Fgf, Cxcr4b, Sdf1-α, Lateral line primordium, Zebrafish

INTRODUCTION

Collective cell migration is a crucial aspect of tissue morphogenesis, repair and cancer metastasis, in which cells retain contacts with each other and move as a coherent assembly with front and rear properties (Friedl and Gilmour, 2009). The path taken by the migrating cells is controlled by the coordinated effects of multiple attractive and repulsive cues. Among many guidance signals, the best known are chemokines, such as stromal cell-derived factor-1 (Sdf1α; Cxcl12), which acts as a chemoattractant for many cell types through activation of its receptors Cxcr4b and Cxcr7b (Tiveron and Cremer, 2008; Sun et al., 2010).

The posterior lateral line in zebrafish has emerged as a powerful paradigm to study directional collective cell migration. The posterior lateral line arises from a cranial placode that forms sensory neurons and a primordium that migrates as a cohesive group towards the tail, depositing the future neuromasts at intervals. The directional migration requires Cxcr4b, expressed in the primordium; Sdf1α, which is present along its path (David et al., 2002; Li et al., 2004; Haas and Gilmour, 2006); and Cxcr7b, which is expressed in the trailing part of the primordium and possibly acts as a sink for ligand (Dambly-Chaudiere et al., 2007; Valentin et al., 2007; Boldajipour et al., 2008). Fibroblast growth factor (Fgf) signalling is required for epithelial morphogenesis and patterning within the primordium (Nechiporuk and Raible, 2008; Lecaudey et al., 2008; Aman and Piotrowski, 2008). The canonical Wnt pathway in the leading primordium induces and restricts Fgf signalling to the trailing zone, which in turn restricts Wnt signalling to the front. This double-feedback cross-talk underlies the polarised expression of chemokine receptors that is required for collective migration of the primordium (Aman and Piotrowski, 2008).

Division of Developmental Neurobiology, MRC National Institute for Medical Research, London NW7 1AA, UK.

*Author for correspondence (qxu@nimr.mrc.ac.uk)

Accepted 11 April 2012

Although previous studies have uncovered key mechanisms required for the migration of the primordium and for neuromast formation, the early steps in which migration is initiated are poorly understood. We find that prior to the onset of migration, there are clusters of isolated cells caudal to the main primordium that express markers of the lateral line primordium. These cells are retained in position such that they fuse with the migrating primordium and contribute to the leading zone and later to the terminal neuromasts. We show that this retention of the isolated cells requires Fgf signalling that mediates attraction towards the primordium, thus counteracting caudal chemoattraction by Sdf1α. The formation of a single cohesive primordium is thus established by opposing chemoattractive signals that act on the initially isolated cell clusters.

MATERIALS AND METHODS

Strains

Cldnb:lyngfp and *cxcr4b/odyseus*(*ody*^{JI049}) strains were provided by D. Gilmour (Haas and Gilmour, 2006). *hsp70:dn-fgfr1* line was used as previously described (Gonzalez-Quevedo et al., 2010).

In situ hybridisation and immunostaining

Whole-mount in situ hybridisation was performed as described (Xu and Wilkinson, 1998) with digoxigenin-labelled RNA probes synthesised according to the manufacturer's instructions (Roche, Boehringer Mannheim). Detection with fluorescent substrate was performed using the Tyramide TSA-Plus Palette System (Perkin Elmer). GFP was detected with anti-GFP (Torrey Pines Biolabs) and anti-rabbit FITC-conjugated antibodies (Jackson ImmunoResearch).

Morpholino knockdowns

Morpholinos were obtained from Gene Tools LLC, Oregon. The Cxcr4b and Cxcr7b morpholinos were used as described (Li et al., 2004; Valentin et al., 2007; Boldajipour et al., 2008). The sequence of the additional Cxcr7b morpholino used is 5′-GGTAATGAGATTCCGATGCCTGGAG-3′. Control morphants correspond to sibling embryos injected with equal doses of the standard control morpholino provided by Gene Tools. To avoid any toxicity effect, 4 ng of morpholino was co-injected with 8 ng of p53 morpholino (Robu et al., 2007; Gerety and Wilkinson, 2011).

Confocal time-lapse imaging

Cldnb:lyngfp embryos were dechorionated, anaesthetised in 0.01% tricaine (Sigma) and mounted in 3% methylcellulose in 0.65× Danieau's solution. When needed, embryos were injected with 80 pg H2B-RFP mRNA. Movies were recorded at 24°C under a Leica DMIRE2 SP2 upright confocal microscope. Cells were manually tracked using the Fiji software.

Heat-shock and SU5402 treatments

hsp70:dn-fgfr1 embryos were heat-shocked at the 16 somite (s) stage for 45 minutes at 37°C and fixed at 24s for analysis. Embryos were treated with 50 µM SU5402 or 0.05% DMSO from 16s to 24s. For live imaging during drug treatment, embryos were pre-treated with 50 µM SU5402 for 2 hours and mounted in the same solution. *pea3* expression in the primordium (Lecaudey et al., 2008) or *hmx3* expression in the otic placode (Feng and Xu, 2010) were used to assess efficiency of the inhibition.

Cell transplantation

Donor embryos were co-injected with LFD (lysine-fluorescein-dextran, Invitrogen) and 50 pg of capped mRNA encoding Fgf10 or tdTomato. Cells were transplanted into wild-type embryos at 50% epiboly stage. The embryos were analysed at 24s by in situ hybridisation for *hmx3* followed by anti-fluorescein (Roche) immunostaining. Embryos showing transplanted cells in the neural tube and/or skin dorsal to the primordium region were selected for further analysis.

Kaede photoconversion

Embryos were injected with 80 pg Kaede mRNA, mounted as described above and photoactivation performed using 30 successive scans with a DPSS 405 nm laser on a Leica DMIRE2 SP2 upright confocal microscope.

Laser ablation

Cldnb:lyngfp embryos were injected with 80 pg H2B-RFP mRNA and mounted as described above. Laser ablation was performed with a VSL-337ND-S nitrogen laser (Spectra-Physics) on a Carl Zeiss Axiovision microscope. Pulses lasting 5-10 seconds were applied on the cells. The primordium region was analysed 2 hours after ablation under a Leica DMIRE2 SP2 upright confocal microscope to select embryos in which separate primordial cells (SPCs) showed fragmented DNA labelled with H2B-RFP.

Statistical analysis

All graphs show means ± s.e.m. SPC frequency graphs represent data collected from at least four independent experiments. *P* values correspond to two-tailed Student's *t*-test analysis, except in Fig. 5D, where the ANOVA and Tukey's post-hoc test were applied.

Quantification

The distance covered by the primordium tip and SPCs in *hsp70:dn-fgfr1*, SU5402-treated and control embryos was quantified after *hmx3* in situ hybridisation at 24s. Each somite was sub-divided into five portions in order to assign a precise position for the tip of main primordium and SPCs in each embryo. The average position represents the distance travelled by these two groups of cells (Fig. 5B; supplementary material Fig. S3).

To quantify the effect of Fgf10 in transplantation experiments, the distance between SPC clusters and the horizontal somitic midline was measured in each embryo using the Fiji software. Distances were transformed into positive and negative values when SPCs were dorsal and ventral to the midline, respectively. The resulting graph is shown in Fig. 6B.

RESULTS

Identification of isolated cells that later fuse with the main primordium

The posterior lateral line placode can be first recognised under Nomarski optics by the 20-somite (s) stage and the primordium starts its migration at 22s (Kimmel et al., 1995; Ghysen and Dambly-Chaudiere, 2007). To understand better the events that precede the onset of migration, we analysed expression of markers of the

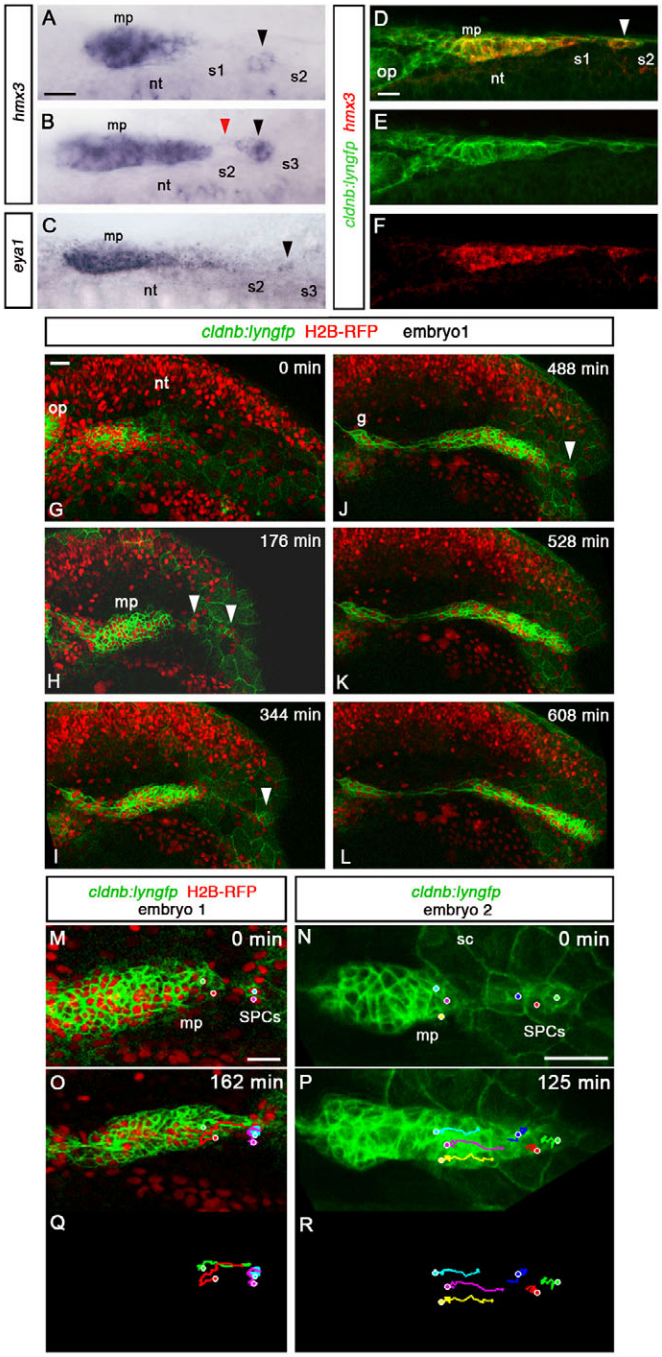

Fig. 1. SPCs have placode identity and fuse with the main primordium. All images are lateral views, anterior to the left, except A-F which show dorsal views. (**A**,**B**) *hmx3* expression in the primordium at 22-24s. Black arrowheads indicate SPCs; the red arrowhead indicates fusion between SPCs and main primordium. (**C**) *eya1* expression in SPCs (black arrowhead) at 20s. (**D-F**) Fluorescence detection of *hmx3* mRNA (red) in *cldnb:lyngfp* (green) embryos at 20s. White arrowhead indicates SPCs. (**G-L**) Images from time-lapse microscopy performed from 18s on a *cldnb:lyngfp* embryo injected with H2B-RFP mRNA (supplementary material Movie 1). White arrowheads indicate SPCs. (**M-R**) Tracking of SPCs and primordium tip cells in embryo 1 (supplementary material Movie 1) and embryo 2 (supplementary material Movie 2) before the fusion. Dots in M and N indicate initial positions of tracked cells. O-R show final time points. g, posterior lateral line ganglion; mp, main primordium; nt, neural tube; op, otic placode; s, somite, sc, skin cells. Scale bars: 25 µm.

posterior lateral line placode and migrating primordium, *hmx3* (Adamska et al., 2000; Feng and Xu, 2010), *eya1* (Kozlowski et al., 2005), and the *cldnb:lyngfp* transgenic line (Haas and Gilmour, 2006). This revealed the presence of one or more small clusters of cells expressing *hmx3* that are located posterior to and clearly separate from the main body of the primordium between 10s and 26s (Fig. 1A,B; supplementary material Fig. S1). These cell clusters express the placodal marker *eya1* and are labelled by *cldnb:lyngfp* (Fig. 1C-F). These cells thus have a lateral line primordium identity, and we refer to them as separate primordial cells (SPCs).

SPCs were rarely seen after 24s, suggesting that they either die, fuse with the main primordium or migrate to another location. No apoptotic cells were detected in this region (not shown), whereas the pattern of *hmx3* expression suggested that SPCs are fusing with the primordium at ~24s, supporting the coalescence hypothesis (Fig. 1B). To distinguish these possibilities unequivocally, we performed time-lapse imaging on *cldnb:lyngfp* embryos (n=7). At 18s, the primordium could be identified as a large cluster of cells extending to somite 1 (Fig. 1G). Time-lapse studies revealed the existence of small groups of Gfp-positive cells located caudal to the primordium (Fig. 1H-J; supplementary material Movies 1, 2). The primordium sequentially coalesced with these clusters and continued its migration (Fig. 1G-L; supplementary material Movies 1, 2), confirming the fusion hypothesis. Tracking analysis of the SPCs and primordium tip cells indicated that the fusion is a consequence of the forward (caudal) movement of the main primordium, rather than backward (rostral) movement of SPCs (Fig. 1M-R; supplementary material Movies 1, 2). To analyse the effect of fusion further, we tracked cells in three regions of the main primordium (leading edge, middle and trailing edge) for 1 hour before and after the fusion. The coalescence with the proximal clusters of SPCs correlated with an increase in speed in the leading two-thirds of the primordium (supplementary material Fig. S1).

To examine in more detail the behaviour of SPCs, we took advantage of the Cxcr7b morpholino (Mo)-mediated knockdown condition, in which the primordium is unable to initiate forward movement (Valentin et al., 2007; Dambly-Chaudiere et al., 2007). We observed variable phenotypes with delayed or ventral migration in Cxcr7b morphants (not shown), as previously described (Valentin et al., 2007). At 28 hours post-fertilisation (hpf), 10% of Cxcr7b morphants (n=206) showed a split phenotype, with a complete migration block and an SPC cluster caudal to the main primordium (supplementary material Fig. S2), whereas control embryos never have a split primordium at this stage. We interpret this phenotype as resulting from an absence of coalescence between the main primordium and SPCs. Live imaging in Cxcr7b morphants (n=6) showed that SPCs are highly protrusive and motile, but fail to make significant forward or backward movements (supplementary material Fig. S2 and Movies 3, 4).

Cxcr4b mediates caudal attraction of SPCs

Directional caudal migration of the primordium is controlled by the guidance receptors Cxcr4b and Cxcr7b. As SPCs express markers of primordial cell identity, this raises the possibility that they too are subject to Sdf1α-mediated chemoattraction. We therefore analysed the expression of the chemokine receptors and ligand Sdf1α at early stages. SPCs express *cxcr4b* from 18s (Fig. 2C-E), *sdf1α* expression in the somites starts at the same stage (Fig. 2A), but *cxcr7b* is only detected at 26s in the trailing part of the primordium and is never seen in the location of SPCs (Fig. 2B).

We addressed next the effect of loss-of-function of Cxcr4b on SPCs. We analysed *hmx3* expression at 24s in homozygous *ody* (*cxcr4b*) mutants and stage-matched controls (Fig. 3A), and calculated the frequency of SPCs, defined as the proportion of embryo sides in which SPCs could be identified at this stage. SPC frequency was significantly decreased in *ody* mutants (Fig. 3B). This effect is not due to the death of Cxcr4b-deficient SPCs, as no increase in apoptosis was detected in *ody* embryos (not shown). Live imaging of *ody* mutants (n=5) and cell tracking revealed that the SPCs move backwards and fuse with the immobile main primordium (Fig. 3C-J; supplementary material Movie 5). A simple model to explain these findings is that, as for the main primordium, Cxcr4b mediates a caudal chemoattraction of SPCs, probably

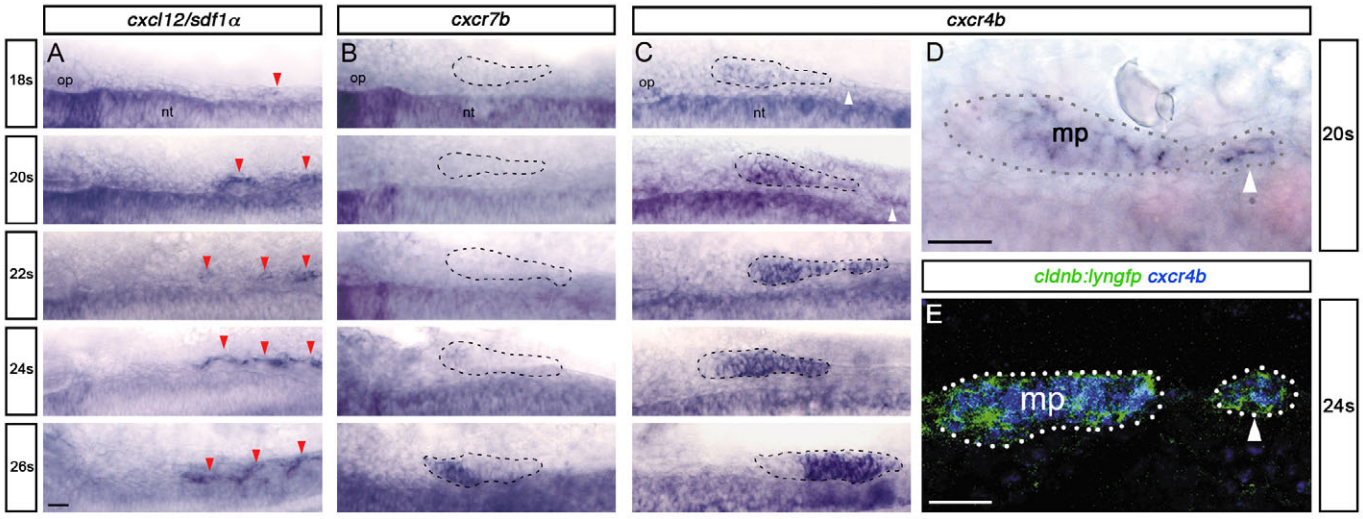

Fig. 2. SPCs express Cxcr4b, but not Cxcr7b. (**A-C**) Time course of *cxcl12/sdf1α* (A), *cxcr7b* (B) and *cxcr4b* (C) expression at 18s-26s. Red arrowheads indicate *sdf1α* expression in somites; white arrowheads indicate *cxcr4b* expression in SPCs. The main primordium (18 and 20s) and primordium fused with SPCs (22 to 26s) are outlined with dashed lines. (**D**,**E**) High magnification views of *cxcr4b* expression at 20s (D) and *cxcr4b* (blue) in *cldnb:lyngfp* embryos (green) at 24s (E). Main primordium (mp) and SPCs are outlined. Scale bars: 25 μm.

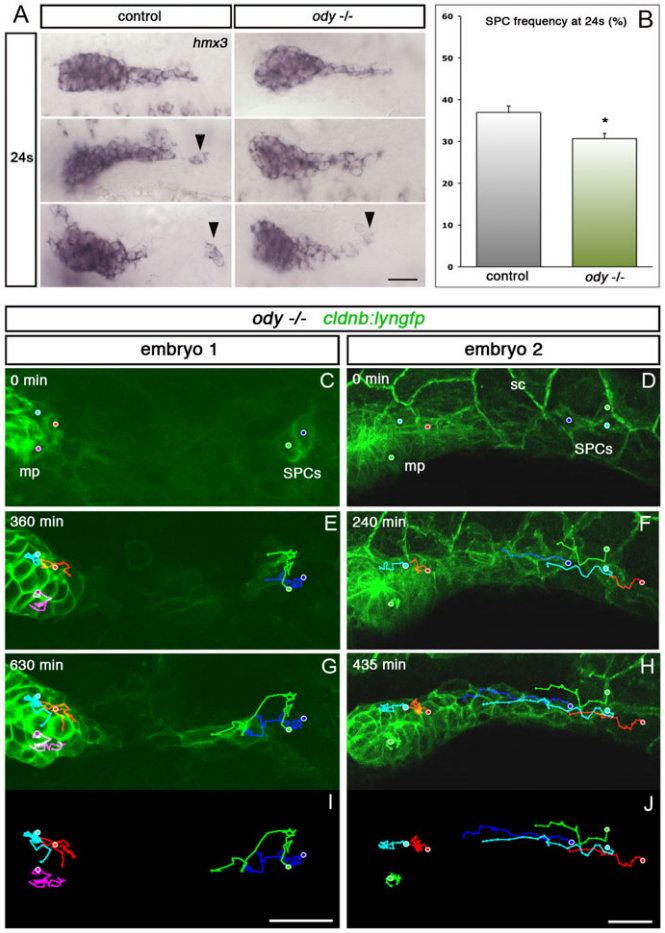

Fig. 3. Cxcr4b attracts SPCs caudally. (**A**) *hmx3* expression at 24s in control and *ody*$^{-/-}$ embryos. Black arrowheads indicate SPCs. (**B**) SPC frequency analysed by *hmx3* expression in *ody*$^{-/-}$ and stage-matched controls at 24s. **P*=0.013. Error bars indicate s.e.m. (**C-J**) Tracking of the SPCs and primordium tip cells in two *ody*$^{-/-}$ embryos (supplementary material Movie 5). In C and D, dots show initial positions of tracked cells. E and F show intermediate time points and G-J show final time points. Scale bars: 25 µm.

through the sensing of Sdf1α; however, this effect is normally counter-balanced by attraction towards the main primordium, which is revealed only when Cxcr4b signalling is impaired.

Fgf signalling attracts SPCs towards the main primordium

A previous study revealed a patterning role for Fgf signalling within the migrating primordium, in which it restricts Wnt activity to the leading zone, thereby indirectly regulating the asymmetric expression of chemokine receptors required for cell migration (Aman and Piotrowski, 2008). Because in other tissues Fgfs act as chemoattractive signals (Sutherland et al., 1996; Sato et al., 2011; Kadam et al., 2012), we considered the possibility that Fgfs also have a more direct role in lateral line cell migration. We analysed the expression of Fgf signalling components and found that after the fusion between the SPCs and primordium, *fgf3* and *fgf10* are expressed in the leading zone, and *fgfr1* in the trailing zone, as previously reported (Fig. 4B) (Nechiporuk and Raible, 2008; Lecaudey et al., 2008; Aman

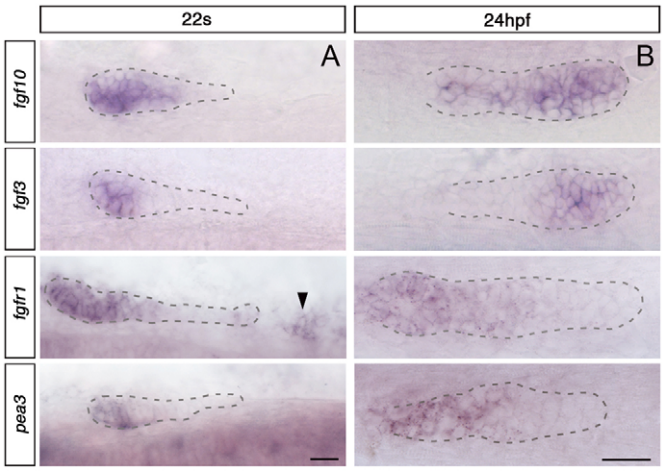

Fig. 4. Expression pattern of Fgf signalling components before and after the fusion. (**A**) Expression of Fgf signalling components at 22s, before fusion. Main primordium is outlined with dashed lines; the black arrowhead indicates SPCs. Dorsal view. (**B**) Expression of Fgf components at 24 hpf, after fusion. The primordium fused with SPCs is outlined with dashed lines. Side view. Scale bar: 25 µm.

and Piotrowski, 2008). However, the expression pattern is strikingly different before fusion, when *fgf3* and *fgf10* are expressed in the back of and throughout the main primordium, respectively, but barely detectable in SPCs, and the receptor *fgfr1* is expressed in the main primordium and in SPCs (Fig. 4A). Thus, the expression of Fgf signalling components is dynamic and switches during the fusion.

We hypothesised that Fgf ligands produced by the main primordium could act as chemoattractive cues for the Fgfr1-expressing SPCs, thus mediating the backward migration in Cxcr4b-deficient embryos. To test this hypothesis, we utilised the *hsp70:dn-fgfr1* line which allows heat shock-induced expression of a dominant-negative form of Fgfr1 (dn-fgfr1) (Lee et al., 2005). Blocking Fgfr activation from 16s led to a higher SPC frequency at 24s (Fig. 5A). Quantification of the distance covered by the tip of the main primordium and SPCs showed that the increased SPC frequency in *hsp70:dn-fgfr1* embryos is mainly due to a forward shift in SPC position, rather than a defect in migration of the main primordium (Fig. 5B; supplementary material Fig. S3).

As the dn-fgfr1 protein is fused with Gfp, we could not use this approach to visualise effects on the dynamic behaviour of cells, and therefore used the Fgfr inhibitor SU5402 in *cldnb:lyngfp* embryos. Treated embryos showed an increase in SPC frequency at 24s, although milder than when the *hsp70:dn-fgfr1* line is used (supplementary material Fig. S3). Quantification of the distance travelled by the main primordium and SPCs at 24s revealed a forward shift in SPC position upon SU5402 treatment, with no significant change in main primordium migration at this stage, as also observed in *hsp70:dn-fgfr1* embryos (supplementary material Fig. S3). Live imaging of SU5402-treated embryos (*n*=3) showed that SPCs underwent a forward movement before being eventually caught up by the main primordium (Fig. 5C; supplementary material Movie 6). After normal initiation of the migration, the primordium stopped its movement at around 24 hpf (data not shown), consistent with the migration defect previously reported (Nechiporuk and Raible, 2008; Lecaudey et al., 2008). As SPC

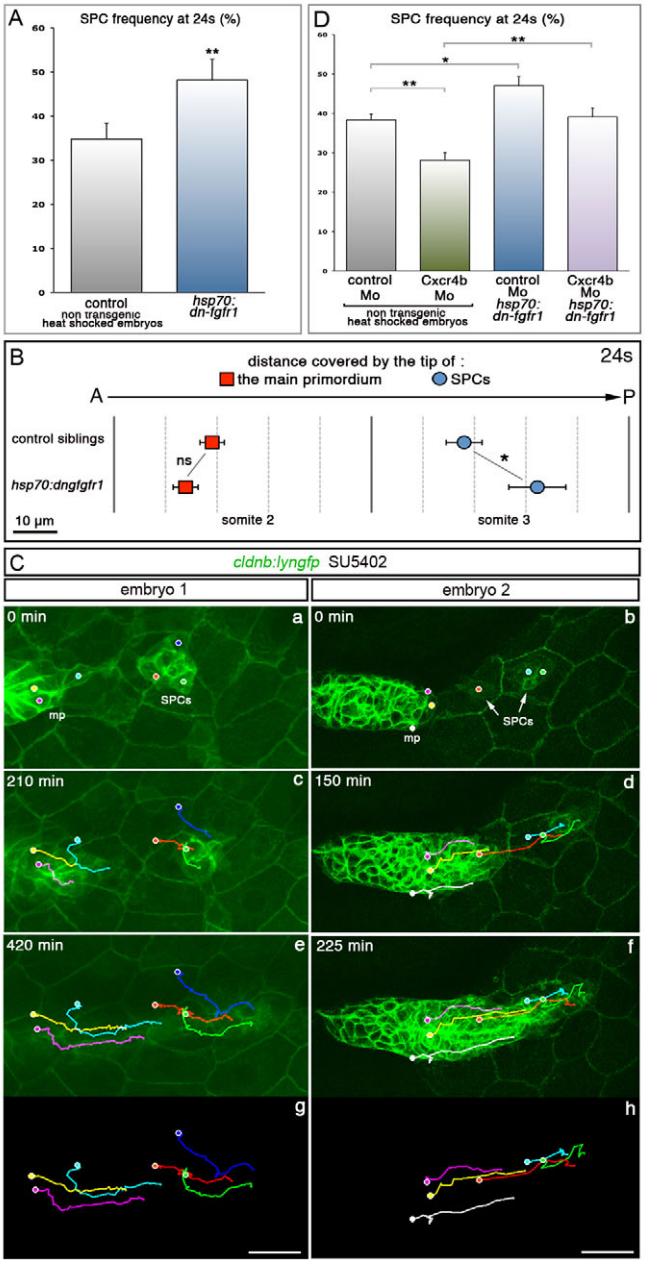

Fig. 5. Fgf signalling attracts SPCs towards the primordium. (**A**) SPC frequency in *hsp70:dn-fgfr1* embryos, heat-shocked at 16s and fixed at 24s, compared with heat-shocked siblings. ***P*=0.008. (**B**) Average distances covered by the tip of the main primordium (red) and SPCs (blue) in *hsp70:dn-fgfr1* embryos (*n*=94) and control siblings (*n*=87) at 24s. See also supplementary material Fig. S3 and Materials and methods. **P*=0.034, ns, non significant (*P*=0.13). (**C**) Tracking of SPCs and primordium tip cells in two SU5402-treated embryos (supplementary material Movie 6). Dots show initial positions of tracked cells in **a** and **b**. **c** and **d** show intermediate time points and **e-h** show final time points. (**D**) SPC frequency in embryos injected with control or Cxcr4b morpholinos in *hsp70:dn-fgfr1* embryos and heat-shocked siblings. Embryos were heat-shocked at 16s and fixed at 24s. **P*<0.05, ***P*<0.01 (ANOVA followed by Tukey's test). Error bars represent s.e.m.

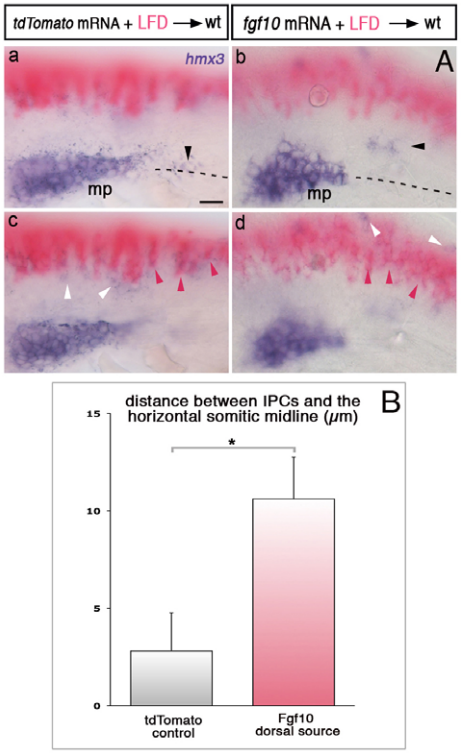

Fig. 6. Ectopic sources of Fgf10 attract SPCs. (**A**) *hmx3* expression (purple) in embryos transplanted with Fgf10- or tdTomato-expressing cells (pink). Black, pink and white arrowheads show SPCs, transplanted cells and *hmx3*-expressing spinal cord neurons, respectively. Dashed lines represent the somitic midlines. *z*-focus made on the primordium and SPCs (**a**,**b**) and on the transplanted cells in the dorsal neural tube (**c**,**d**). (**B**) Distance between SPCs and the horizontal somitic midline in embryos with transplanted cells expressing Fgf10 (*n*=46) or tdTomato (*n*=38) dorsal to the primordium region. **P*=0.010. See also supplementary material Fig. S3 and Materials and methods. Error bars represent s.e.m. Scale bars: 25 µm.

clusters do not express Cxcr7b, their forward migration might not be sustained, but the fusion with the main primordium precludes analysis of their longer term behaviour. We therefore blocked Fgf signalling with SU5402 in Cxcr7b morphants, in which fusion is prevented. Live imaging revealed that SPCs migrate a short distance forward but then stop their progression (data not shown), consistent with a requirement for Cxcr7b for persistent directional migration.

We analysed next whether the backward migration of SPCs observed in Cxcr4b-deficient embryos is mediated by the Fgf pathway. To inactivate Fgf signalling in Cxcr4b-deficient embryos, we used *hsp70:dn-fgfr1* embryos which were injected with Cxcr4b Mo. As observed in *ody* mutants, Cxcr4b morphants displayed a reduced SPC frequency, confirming the efficiency and specificity of the Cxcr4b Mo (Fig. 5D). Blocking of Fgfr activation prevented the backward migration of SPCs seen in Cxcr4b morphants (Fig. 5D).

To investigate whether Fgf ligands are sufficient to mediate SPC attraction, we transplanted Fgf10- or control tdTomato-expressing cells into wild-type hosts and analysed the position of SPCs. SPCs were found to have deviated towards ectopic dorsal sources of Fgf10 (Fig. 6; supplementary material Fig. S3), indicating that Fgf10 is sufficient to attract SPCs. As primordium cells also express Fgfr1 (Fig. 4), it was possible that they too respond to ectopic Fgf expression. We occasionally observed cells of the main primordium that slightly deviated towards

dorsal sources of Fgf10 (not shown), but most primordium cells stayed in place. Our interpretation of this result is that cells of the main primordium themselves produce high levels of Fgf ligands and are, therefore, less sensitive to ectopic sources of Fgf10 than the SPCs, which are located further away from endogenous sources of Fgf10 and Fgf3. Taken together, these results show that Fgf signalling from the primordium attracts SPCs, which, by counter-balancing the caudal attraction to Sdf1α, keeps them in place so that they fuse with the main primordium once it initiates migration.

SPCs remain in the leading zone and contribute to the terminal neuromasts

To analyse the contribution of SPCs to the lateral line, we conducted fate-mapping experiments using Kaede photoconversion (Hatta et al., 2006). Kaede-expressing SPCs (Fig. 7Aa,b) or a region containing SPCs (supplementary material Fig. S4) were photoconverted from green to red before the fusion. In most embryos (82%, *n*=17), red cells were found in the leading zone of the primordium (Fig. 7Ac,d; supplementary material Fig. S4) and later contributed to the last three neuromasts (Fig. 7Ae,f; supplementary material Fig. S4). Activation of a region containing all of the SPCs revealed that the leading zone contains cells derived both from SPCs and the initial main body of the primordium; these cell populations intermingle in the leading zone (supplementary material Fig. S4).

We next performed laser-ablation experiments. Owing to bleaching of Gfp fluorescence upon laser application, we were unable to carry out repeated ablations in the same embryo to remove the whole population of SPCs. However, partial ablation of SPCs before the fusion led to impairment of the terminal phase of migration (71% embryos, *n*=14), consistent with the results of fate mapping. Upon arriving in the tail region, the primordium was smaller, stopped before the normal end point and failed to split to form the terminal neuromasts (Fig. 7B). The formation and the deposition of more anterior neuromasts was not affected (Fig. 7B), and their shape and organisation appeared normal (not shown). Taken together, these data show that SPCs are crucial for formation of the terminal neuromasts.

DISCUSSION

The posterior lateral line primordium has been widely studied as a model for how a group of cells undergoes collective migration. We found that at early stages, prior to the onset of migration, cells with primordium identity are not organised in a single group. Rather, there is a subpopulation of future lateral line cells, SPCs, that are located caudal to the main primordium. Because SPCs express the Cxcr4b chemokine receptor, as for the cells in the main primordium, they are subject to chemoattraction that would cause them to migrate caudally. Such caudal migration would prevent or delay the SPCs from meeting the main primordium such that they can fuse to form a single cluster, a necessary step for the

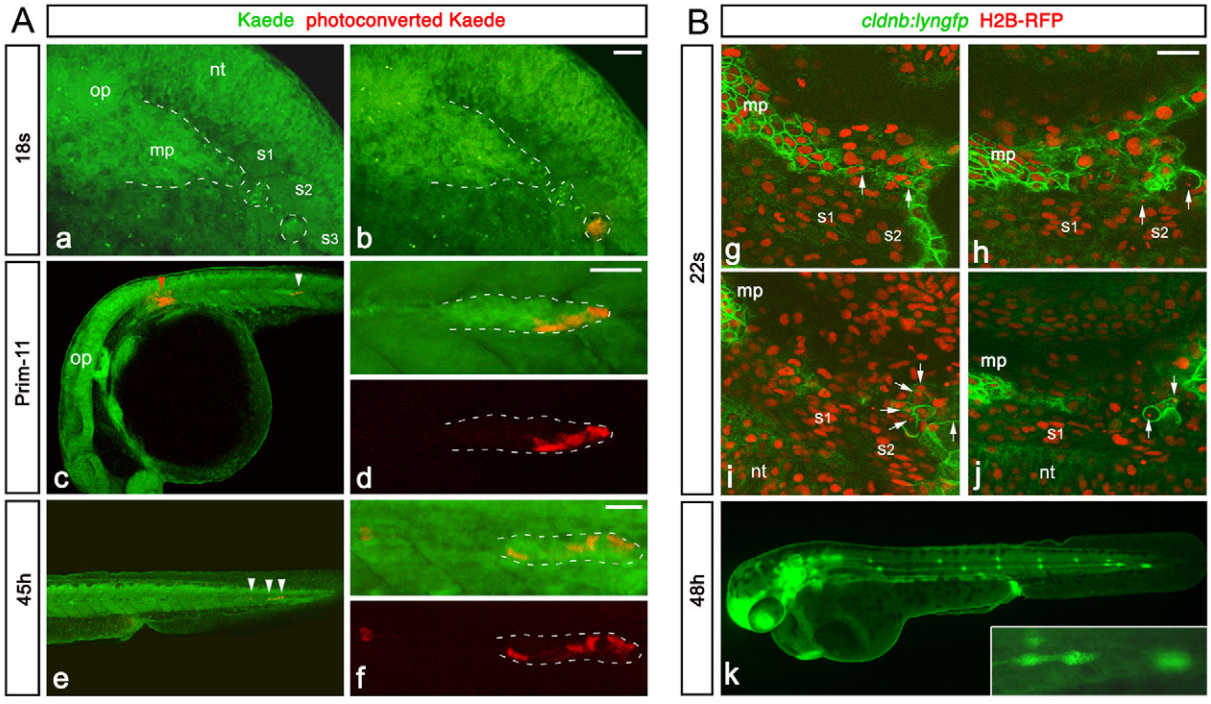

Fig. 7. Progeny of SPCs contributes to the terminal neuromasts. (**Aa**,**Ab**) Primordium region of 18s embryo injected with Kaede mRNA, before (a) and after (b) photoactivation in the most caudal SPC cluster. The main primordium and SPCs are outlined with dashed lines. (**Ac**) Low magnification of the same embryo at prim-11, showing red cells (white arrowhead) in the migrating primordium. No deposited red cell is observed between the region of activation (red arrowhead) and the primordium. (**Ad**) High magnification of the primordium shown in c, showing red cells in the leading part of the primordium. (**Ae**) Low magnification of the trunk at 45h, showing red cells (white arrowheads) in the last deposited neuromast and in the primordium reaching the tail. No red cell is deposited more anteriorly. (**Af**) High magnification of the primordium and the terminal neuromast shown in e. See also supplementary material Fig. S4. (**Bg-Bj**) Examples of confocal sections showing the primordium region of *cldnb:lyngfp* embryos at 22s, 2 hours after partial laser ablation of SPCs. H2B-RFP-labelled fragmented DNA of dying SPCs is indicated by white arrows. (**Bk**) Phenotype observed at 48h in embryos in which a subset of SPCs were laser-ablated on the left side. The primordium is small and unable to complete its journey, compared with the control non-ablated side. The inset shows a high magnification of the arrested primordium. mp, main primordium; nt, neural tube; op, otic placode; s, somite. Scale bars: 25 μm.

coordinated collective migration. We show that the formation of single primordium is achieved by two distinct guidance cues that counteract each other to position the SPCs.

Roles of Sdf1α and Fgf signalling

We find that disruption of Sdf1α/Cxcr4b or Fgf signalling elicits backward or forward migration of SPCs, respectively, and that inhibition of Fgf signalling blocks the backward migration that would otherwise occur in the absence of Cxcr4b. In addition, ectopic sources of Fgf ligands can attract SPCs. We therefore propose the following model (Fig. 8). The balance between the Sdf1α/Cxcr4b and Fgf3/10/Fgfr1 signalling normally leads to an absence of anteroposterior directional movement of SPCs, such that the migrating primordium meets and fuses with them. However, if SPCs are unable to sense Sdf1α, they migrate back towards the Fgf-producing main primordium in an Fgfr1-dependent manner. By contrast, compromising Fgf signalling releases the SPCs from Fgf-mediated chemoattraction, resulting in their Cxcr4b-dependent short distance forward migration on the Sdf1α-expressing path. Lack of Cxcr7b in SPCs prevents their long-term directional forward migration. These opposite movements reveal a tug of war between two guidance signals, which maintain the position of SPCs.

The classic transcriptional readout of the Fgf pathway, *pea3*, is expressed in the back of the primordium from around 20s, but could not be detected in SPCs (Fig. 4). It is possible that *pea3* expression is too low in SPCs to be detected by in situ hybridisation. Alternatively, Fgfr1 activation in these cells could regulate migration independently of *pea3* by acting more directly on cytoskeletal dynamics and small GTPases. The signalling events mediating Fgf chemotactic effects in other systems remain poorly understood (Dormann and Weijer, 2006; Dorey and Amaya, 2010) and might not involve transcriptional activation of target genes.

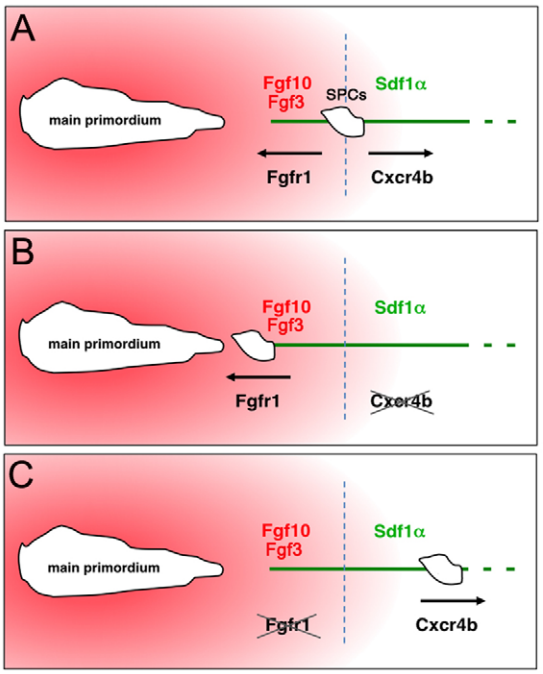

Fig. 8. Model of opposing effects of Sdf1α/Cxcr4b and Fgf signalling on SPCs. (**A**) In the normal situation, a balance between Sdf1α/Cxcr4b and Fgf/Fgfr1 signalling leads to no net forward or backward movement of SPCs. (**B**) Cxcr4b-deficient SPCs are unable to sense the Sdf1α chemokine and therefore migrate towards the Fgf-secreting main primordium. (**C**) Inhibition of Fgf signalling releases the chemoattraction of SPCs, resulting in their Cxcr4b-dependent short distance forward migration on the Sdf1α path. These opposite movements reveal a tug of war between the two signalling systems, whereby Fgf-mediated chemoattraction retains SPCs in position to facilitate their fusion with the main primordium.

Origin and roles of SPCs

This is, to our knowledge, the first report of cells with placodal identity that are isolated from the main primordium and located beyond somite 1, which was thought to be the caudal limit of the primordium at the early stages (Kimmel et al., 1995; Dambly-Chaudiere et al., 2007; Sarrazin et al., 2010). SPCs are observed by *hmx3* expression from 10s onwards, well before Cxcr4b and Sdf1α start to be expressed, and can also be detected in *ody* mutants at these early stages (supplementary material Fig. S1). Thus, SPCs do not come from a premature Cxcr4b-dependent caudal migration of posterior lateral line placodal cells. One possibility is that SPCs could have a developmental origin that is different from other cells of the posterior lateral line placode. A recent study uncovered the contribution of neuroepithelial cells to the otic placode (Freyer et al., 2011), showing that cells from distinct embryonic territories can contribute to placode formation and morphogenesis. However, it seems unlikely that SPCs have a distinct embryonic origin, as they express the same placodal markers as the main primordium. It is believed that cranial placodes arise from a horseshoe-shaped pan-placodal domain at the border between the anterior neural plate and non-neural ectoderm (Schlosser, 2010). The posterior lateral line placode is the most posterior cranial placode. The SPCs thus represent the most posterior placodal cells and could be a consequence of a fuzzy posterior boundary of the pan-placodal domain. Chemoattraction by Fgf signalling would thus represent a mechanism to ensure that an initial imprecise organisation is transformed into a single migrating primordium.

The migrating primordium is patterned along its anteroposterior axis such that it has a leading-trailing zone asymmetry in cell behaviour and gene expression (Nechiporuk and Raible, 2008; Lecaudey et al., 2008; Aman and Piotrowski, 2008). Of particular interest is the possibility that the leading zone cells could be similar to tip cells described in other migratory systems, including germ cells in *C. elegans* (Cinquin et al., 2010), and trachea in *Drosophila* (Sutherland et al., 1996; Uv et al., 2003). Tip cells located at the front exert an organisational effect over other cells that migrate in their wake and are essential for successful group migration to occur. The fusion of SPCs with the main primordium correlated with a speeding up of migration. The premature arrest of migration following partial SPC ablation could be due to the decreased number of progenitors in the leading zone of the primordium (McGraw et al., 2011; Valdivia et al., 2011), or a specific role of SPCs in migration. Fate-mapping revealed that SPCs stay in the leading zone of the primordium during the whole course of the migration. Interestingly, photoconversion of Kaede in cells in the leading primordium after the fusion (Nechiporuk and Raible, 2008) labelled neuromasts that are more anteriorly located than those that we find receive a contribution from SPCs. Thus, cells derived from the SPCs seem to remain a distinct population of leading zone cells that are deposited to form the posterior-most neuromasts.

Later roles of Fgf signalling

Fgf signalling is required for several important aspects of lateral line morphogenesis, neuromast formation and the correct migration of the primordium (Lecaudey et al., 2008; Nechiporuk and Raible,

2008; Aman and Piotrowski, 2008). Previous studies have shown that blocking Fgf signalling disrupts the normal polarity of the primordium, including the restricted expression of chemokine receptors that is required for migration. It has thus been proposed that the primary role of Fgf signalling is in patterning within the primordium, which in turn is required for correct migration. Our findings suggest a model in which Fgfs also have a more direct role in coordinating cell migration. If the role of Fgfs in chemoattraction we have uncovered continues at later stages, Fgf ligands produced by the cells in the leading zone might act to attract Fgfr1-expressing cells in the trailing part. Consistent with this, blocking the Fgf pathway leads to elongated morphology of the primordium and uncoordinated migration (Lecaudey et al., 2008). Aman and Piotrowski (Aman and Piotrowski, 2008) reported normal coordinated primordium migration in transgenic *hsp70:dkk1* embryos, in which both Wnt and Fgf signalling are impaired. However, in such a situation, the loss of Fgf signalling might be compensated for by other events downstream of Wnt inactivation. Alternatively, the chemoattractive role of Fgfs might be transient, and downregulated after fusion of SPCs with the main primordium, when the expression patterns of some Fgf pathway components change. Distinguishing between these alternatives will require the ability to uncouple the multiple downstream effects of Fgf signalling in the migrating primordium.

In summary, our work reveals a novel role for the Fgf pathway in chemoattraction-mediated assembly of a migrating cell group in the posterior lateral line. It will be interesting to uncover whether similar chemotactic mechanisms could initiate or maintain a compact state of other migratory cell groups during normal development or cancer invasion.

Acknowledgements
We thank Elke Ober for help with the laser ablation experiments and the staff of the NIMR fish facility for their work.

Funding
This study was funded by the Medical Research Council [U117532048]. M.A.B. was supported by Fellowships from the Fondation Fyssen (France) and the European Molecular Biology Organization (EMBO). Deposited in PMC for release after 6 months.

Competing interests statement
The authors declare no competing financial interests.

Supplementary material
Supplementary material available online at
http://dev.biologists.org/lookup/suppl/doi:10.1242/dev.080275/-/DC1

References

Adamska, M., Léger, S., Brand, M., Hadrys, T., Braun, T. and Bober, E. (2000). Inner ear and lateral line expression of a zebrafish Nkx5-1 gene and its downregulation in the ears of FGF8 mutant, ace. *Mech. Dev.* **97**, 161-165.
Aman, A. and Piotrowski, T. (2008). Wnt/beta-catenin and Fgf signaling control collective cell migration by restricting chemokine receptor expression. *Dev. Cell* **15**, 749-761.
Boldajipour, B., Mahabaleshwar, H., Kardash, E., Reichman-Fried, M., Blaser, H., Minina, S., Wilson, D., Xu, Q. and Raz, E. (2008). Control of chemokine-guided cell migration by ligand sequestration. *Cell* **132**, 463-473.
Cinquin, O., Crittenden, S. L., Morgan, D. E. and Kimble, J. (2010). Progression from a stem cell-like state to early differentiation in the *C. elegans* germ line. *Proc. Natl. Acad. Sci. USA* **107**, 2048-2053.
Dambly-Chaudiere, C., Cubedo, N. and Ghysen, A. (2007). Control of cell migration in the development of the posterior lateral line: antagonistic interactions between the chemokine receptors CXCR4 and CXCR7/RDC1. *BMC Dev. Biol.* **7**, 23.
David, N. B., Sapede, D., Saint-Etienne, L., Thisse, C., Thisse, B., Dambly-Chaudiere, C., Rosa, F. M. and Ghysen, A. (2002). Molecular basis of cell migration in the fish lateral line: role of the chemokine receptor CXCR4 and of its ligand, SDF1. *Proc. Natl. Acad. Sci. USA* **99**, 16297-16302.
Dorey, K. and Amaya, E. (2010). FGF signalling: diverse roles during early vertebrate embryogenesis. *Development* **137**, 3731-3742.
Dormann, D. and Weijer, C. J. (2006). Chemotactic cell movement during Dictyostelium development and gastrulation. *Curr. Opin. Genet. Dev.* **16**, 367-373.
Feng, Y. and Xu, Q. (2010). Pivotal role of hmx2 and hmx3 in zebrafish inner ear and lateral line development. *Dev. Biol.* **339**, 507-518.
Freyer, L., Aggarwal, V. and Morrow, B. E. (2011). Dual embryonic origin of the mammalian otic vesicle forming the inner ear. *Development* **138**, 5403-5414.
Friedl, P. and Gilmour, D. (2009). Collective cell migration in morphogenesis, regeneration and cancer. *Nat. Rev. Mol. Cell Biol.* **10**, 445-457.
Gonzalez-Quevedo, R., Lee, Y., Poss, K. D. and Wilkinson, D. G. (2010). Neuronal regulation of the spatial patterning of neurogenesis. *Dev. Cell* **18**, 136-147.
Gerety, S. S. and Wilkinson, D. G. (2010). Morpholino artifacts provide pitfalls and reveal a novel role for pro-apoptotic genes in hindbrain boundary development. *Dev. Biol.* **350**, 279-289.
Ghysen, A. and Dambly-Chaudiere, C. (2007). The lateral line microcosmos. *Genes Dev.* **21**, 2118-2130.
Haas, P. and Gilmour, D. (2006). Chemokine signaling mediates self-organizing tissue migration in the zebrafish lateral line. *Dev. Cell* **10**, 673-680.
Hatta, K., Tsujii, H. and Omura, T. (2006). Cell tracking using a photoconvertible fluorescent protein. *Nat. Protoc.* **2**, 960-967.
Kadam, S., Ghosh, S. and Stathopoulos, A. (2012). Synchronous and symmetric migration of Drosophila caudal visceral mesoderm cells requires dual input by two FGF ligands. *Development* **139**, 699-708.
Kimmel, C. B., Ballard, W. W., Kimmel, S. R., Ullmann, B. and Schilling, T. F. (1995). Stages of embryonic development of the zebrafish. *Dev. Dyn.* **203**, 253-310.
Kozlowski, D. J., Whitfield, T. T., Hukriede, N. A., Lam, W. K. and Weinberg, E. S. (2005). The zebrafish dog-eared mutation disrupts eya1, a gene required for cell survival and differentiation in the inner ear and lateral line. *Dev. Biol.* **277**, 27-41.
Lecaudey, V., Cakan-Akdogan, G., Norton, W. H. and Gilmour, D. (2008). Dynamic Fgf signaling couples morphogenesis and migration in the zebrafish lateral line primordium. *Development* **135**, 2695-2705.
Lee, Y., Grill, S., Sanchez, A., Murphy-Ryan, M. and Poss, K. D. (2005). Fgf signaling instructs position-dependent growth rate during zebrafish fin regeneration. *Development* **132**, 5173-5183.
Li, Q., Shirabe, K. and Kuwada, J. Y. (2004). Chemokine signaling regulates sensory cell migration in zebrafish. *Dev. Biol.* **269**, 123-136.
McGraw, H. F., Drerup. C. M., Culbertson, M. D., Linbo, T., Raible, D. W. and Nechiporuk, A. V. (2011). Lef1 is required for progenitor cell identity in the zebrafish lateral line primordium. *Development* **138**, 3921-3930.
Nechiporuk, A. and Raible, D. W. (2008). FGF-dependent mechanosensory organ patterning in zebrafish. *Science* **320**, 1774-1777.
Robu, M. E., Larson, J. D., Nasevicius, A., Beiraghi, S., Brenner, C., Farber, S. A. and Ekker, S. C. (2007). p53 activation by knockdown technologies. *PLoS Genet.* **3**, e78.
Sarrazin, A. F., Nuñez, V. A., Sapède, D., Tassin, V., Dambly-Chaudière, C. and Ghysen, A. (2010). Origin and early development of the posterior lateral line system of zebrafish. *J. Neurosci.* **30**, 8234-8244.
Sato, A., Scholl, A. M., Kuhn, E. B., Stadt, H. A., Decker, J. R., Pegram, K., Hutson, M. R. and Kirby, M. L. (2011). FGF8 signaling is chemotactic for cardiac neural crest cells. *Dev. Biol.* **354**, 18-30.
Schlosser, G. (2010). Making senses: development of vertebrate cranial placodes. *Int. Rev. Cell Mol. Biol.* **283**, 129-234.
Sun, X., Cheng, G., Hao, M., Zheng, J., Zhou, X., Zhang, J., Taichman, R. S., Pienta, K. J. and Wang, J. (2010). CXCL12 / CXCR4 / CXCR7 chemokine axis and cancer progression. *Cancer Metastasis Rev.* **29**, 709-722.
Sutherland, D., Samakovlis, C. and Krasnow, M. A. (1996). branchless encodes a *Drosophila* FGF homolog that controls tracheal cell migration and the pattern of branching. *Cell* **87**, 1091-1101.
Tiveron, M. C. and Cremer, H. (2008). CXCL12/CXCR4 signalling in neuronal cell migration. *Curr. Opin. Neurobiol.* **18**, 237-244.
Uv, A., Cantera, R. and Samakovlis, C. (2003). *Drosophila* tracheal morphogenesis: intricate cellular solutions to basic plumbing problems. *Trends Cell Biol.* **13**, 301-309.
Valdivia, L. E., Young, R. M., Hawkins, T. A., Stickney, H. L., Cavodeassi, F., Schwarz, Q., Pullin, L. M., Villegas, R., Moro, E., Argenton, F. et al. (2011). Lef1-dependent Wnt/β-catenin signalling drives the proliferative engine that maintains tissue homeostasis during lateral line development. *Development* **138**, 3931-3941.
Valentin, G., Haas, P. and Gilmour, D. (2007). The chemokine SDF1a coordinates tissue migration through the spatially restricted activation of Cxcr7 and Cxcr4b. *Curr. Biol.* **17**, 1026-1031.
Xu, Q. and Wilkinson, D. G. (1998). In situ hybridization of mRNA with hapten labelled probes. In *In Situ Hybridization: A Practical Approach*, 2nd edition (ed. D. G. Wilkinson), pp. 87-106. Oxford: Oxford University Press.